Conformation of Xanthene Dyes in the Sulfhydryl 1 Binding Site of Myosin. 2†

Katalin Ajtai and Thomas P. Burghardt*

Department of Biochemistry and Molecular Biology, Mayo Foundation, Rochester, Minnesota 55905

Received June 14, 1995; Revised Manuscript Received September 27, 1995®

ABSTRACT: The fluorescent dyes 5′-(iodoacetamido)tetramethylrhodamine (5′IATR) and 5′-(iodoacetamido)-fluorescein (5′IAF) bind covalently to the reactive sulfhydryl (SH1) of myosin subfragment 1 (S1), the 5′IATR as a dimer and the 5′IAF as a monomer. The conformation of the dimer and the dye−protein complex was investigated by comparison of several spectroscopic signals of the molecules before and after their association into a complex and interpretation of any changes using a coupled dipole oscillator model adapted for this problem [Burghardt & Ajtai (1995) *Biophys. Chem.* (submitted for publication)]. Absorption and fluorescence spectroscopies were performed on 5′IAF, 5′IATR, and rhodamine 6G (R6G) and rhodamine B (RB) as models of dimer conformation. Absorption, fluorescence, and circular dichroism (CD) spectroscopies were performed on 5′IATR-modified S1 (5′R-S1) and 5′IAF-modified S1 (5′F-S1). Combined spectroscopic and 2-D NMR data from rhodamines in solution determined the conformations of the dimers. Xanthene rings from dimers of identical dyes (homodimers) stacked in two structures having very different spectroscopic signatures. Xanthene rings from the heterodimer of R6G and RB stacked in one conformation. The two homodimer conformations of 5′IATR are equally likely to form in solution. The other rhodamine homodimers have one dominant, but not exclusive, structure. Both conformations of the 5′IATR dimer were coupled to a tryptophan as a model of the dye−protein interaction at SH1. The calculated CD from one dimer conformer (dimer A) coupled to tryptophan is negative for the lowest energy CD absorption band. The other dimer (dimer B) gives positive CD on the two lowest energy CD absorption bands. Both dimer structures of 5′IATR contributed to the early time-dependent CD signal from 5′IATR binding to SH1, but at equilibrium the CD signal indicated only dimer B, suggesting that the SH1 binding pocket converts dimer A into dimer B. The time-dependent CD signal from 5′IAF changes amplitude but not shape during the reaction with SH1. The model calculation accounting for the spectroscopic signals of 5′R-S1 and 5′F-S1 indicates several likely conformations of the 5′IATR dimer−tryptophan and 5′IAF−tryptophan complexes embedded in S1. These structures fit to the α-carbon structure of the SH1 binding pocket when the 5′IATR dimer and 5′IAF interact closely with Trp510 [Rayment et al. (1993) *Science 261,* 50−58]. The additional constraints imposed by the known orientation of the rhodamine dimer relative to the principal hydrodynamic frame of S1 reject all but one of the 5′IATR dimer−tryptophan and 5′IAF−tryptophan structures coordinated with Trp510.

Xanthene dyes probed myosin cross-bridges in muscle fibers in the search for evidence of rotational movement during the active cycle suggested by the rotating cross-bridge model of contraction (Reedy et al., 1965; Huxley, 1969; Huxley & Simmons, 1971). (Iodoacetamido)tetramethylrhodamine (IATR)[1] was useful in this search since it indicated the time course of cross-bridge rotational movement in contraction (Borejdo et al., 1979; Hellen et al., 1995) and identified distinctive actin-bound cross-bridge attitudes in different physiological states of the muscle fiber (Borejdo et al., 1982; Burghardt et al., 1983; Andreev et al., 1993). Subsequently, we utilized the probe in addition to other fluorescent and spin labels to estimate the trajectory of cross-bridge rotation during muscle contraction (Burghardt & Ajtai, 1994; Ajtai et al., 1994). We demonstrated that IATR detected various cross-bridge attitudes because, when modifying myosin, its transition dipole is more nearly orthogonal to an axis of cross-bridge rotation than some of the other dyes or spin labels used to modify myosin and detect cross-bridge rotation. All conclusions concerning the movement of myosin derived from extrinsic probes, including IATR, are based on the reliability of evidence that the probe is specifically and rigidly attached to the myosin. Nearly as important is knowing the probe orientation relative to the protein principal hydrodynamic frame (PHF) axes.

IATR is available in two isomeric forms where the linking iodoacetamido is at the 5′ or 6′ position on the benzoic group of rhodamine giving 5′IATR or 6′IATR. These probes target the reactive thiols on myosin. With investigation of 5′- and 6′IATR specificity and rigidity on SH1 we observed properties of probe conformation. We found that when labeling muscle fibers (i) only the 5′IATR attaches specifically and rigidly to SH1, (ii) when located at SH1 both probes exhibit a stoichiometry of two probes per SH1, and (iii) both probes form dimers in aqueous buffered solution, as do other rhodamine dyes, such that under our labeling conditions a

† This work was supported by National Institutes of Health Grant R01 AR 39288, American Heart Association Grant-in-Aid 930 06610, and the Mayo Foundation.

* To whom correspondence should be sent: phone, 507-284-8120; FAX, 507-284-9349; Email, Burghardt@mayo.edu.

® Abstract published in *Advance ACS Abstracts,* November 15, 1995.

[1] Abbreviations: CD, circular dichroism; DMF, dimethylformamide; FRET, fluorescence resonance energy transfer; IAA, iodoacetamide; NMR, nuclear magnetic resonance; PHF, principal hydrodynamic frame; R6G, rhodamine 6G; RB, rhodamine B; S1, myosin subfragment 1; SH1, sulfhydryl 1 or Cys707 on myosin S1; TME, L-tryptophan methyl ester; TRFAD, time-resolved fluorescence anisotropy decay; 5′IAF, 5′-(iodoacetamido)fluorescein; 5′IATR, 5′-(iodoacetamido)tetramethylrhodamine; 5′F-S1, 5′IAF-labeled S1; 5′R-S1, 5′IATR-labeled S1.

0006-2960/95/0434-15943$09.00/0

significant fraction of the 5′- and 6′IATR molecules are dimeric (Ajtai et al., 1992; Burghardt et al., 1995). These observations suggested that a rhodamine dimer could label SH1 (Ajtai et al., 1992). We report here spectroscopic evidence for the presence and conformation of the 5′IATR dimer bound to SH1, and on a parallel investigation of rhodamine dimer conformation in solution.

We studied the structure of dimers formed from rhodamine 6G (R6G), rhodamine B (RB), 5′IATR, and the heterodimer of R6G + RB with optical spectroscopy and 2-D NMR [NMR data reported in Ilich et al. (1995)] and combined the available data to form conclusions about the dimer structure. We investigated dimerization of rhodamine in solution optically by measuring the effective extinction coefficients as a function of concentration. Analysis of the curves indicates the equilibrium constant for dimer formation and the extinction coefficients for the pure monomer and dimer forms (Rohatgi & Mukhopadhyay, 1971; Selwyn & Steinfeld, 1972; Bloński, 1991). We also measured the fluorescence anisotropy of the rhodamine monomer and dimer (Burghardt et al., 1995). The absorption band energy maxima, absorption dipole strengths, and fluorescence anisotropies of the monomer and dimer molecules are interpreted in terms of the dimer structure using coupled dipole oscillator methods outlined elsewhere (Burghardt & Ajtai, 1995, and referred to subsequently as part I). The dimer conformation is also constrained by 2-D NMR data on proton distances in the monomer and dimer species. We find that the dimers have stacked xanthene rings as indicated previously (Gál et al., 1973; López Arbeloa & Ruiz Ojeda, 1982; Grajek et al., 1986). Identical pair dimers (homodimers) exist in two structures in solution with very different spectroscopic signatures. The 5′IATR dimer has equal probability of existing in either structural form while at the other extreme the R6G dimer is ~90% of the time in a single conformation. The heterodimer pair made from R6G and RB has a single solution structure.

We investigated the interaction of the 5′IATR dimer and 5′IAF with myosin S1. The 5′IATR, the 5′IATR dimer, and the 5′IAF have no circular dichroism (CD) signal in solution (the probes are enantiomeric) or in the presence of myosin when the probe is prevented from chemically modifying SH1. However, when SH1 was modified, the 5′IATR dimer or the 5′IAF interacts with the binding pocket, causing an induced CD signal in the probe absorption band. We observed a complex time dependence in the CD signal when the 5′IATR dimer modifies the protein that indicates an aspect of the dimer−protein interaction. We interpreted the absorption band energy maxima, absorption dipole strengths, the rotary strengths, and fluorescence anisotropies of the two probe molecules in solution and when modifying SH1 in terms of the probe−protein conformation using coupled dipole oscillator methods described in part I. The crystallographic structure of S1 (Rayment et al., 1993) and the orientational constraints imposed by our work indicating the orientation of the rhodamine dimer relative to the PHF of S1 (Ajtai et al., 1994) further constrain the probe−SH1 conformation. These constraints and the requirement that both the 5′IATR dimer and 5′IAF fit into the SH1 binding pocket and give similar fluorescence polarization ratios from muscle fibers allow us to surmise a likely conformation of the protein−dye complex.

MATERIALS AND METHODS

Chemicals. ATP, ADP, P^1,P^5-di-5′-adenosyl pentaphosphate (Ap_5A), phenylmethanesulfonyl fluoride (PMSF), ethylenediaminetetraacetic acid (EDTA), ethylene glycol bis-(β-aminoethyl ether)-*N*,*N*,*N*′,*N*′-tetraacetic acid (EGTA), dithiothreitol (DTT), iodoacetamide (IAA), and dimethylformamide (DMF) were from Sigma (St. Louis, MO). The L-tryptophan methyl ester hydrochloride (TME) and photometric grade glycerol were from Aldrich (Milwaukee, WI). The fluorescent labels 5′-(iodoacetamido)tetramethylrhodamine (5′IATR) and 5′-(iodoacetamido)fluorescein (5′IAF) were from Molecular Probes (Eugene, OR). The dyes 2-[6-(ethylamino)-3-(ethylimino)-2,7-dimethyl-3*H*-xanthen-9-yl]-benzoic acid ethyl ester (rhodamine 6G or R6G) and 2-[6-(ethylamino)-3-(ethylimino)-3*H*-xanthenyl]benzoic acid (rhodamine B or RB) were from Kodak (Rochester, NY). All chemicals were of analytical grade.

Solutions. The dyes without reactive groups were directly dissolved in water at 0.01, 0.10, 0.20, and 0.40 mM probe concentrations or at 1 μM probe concentration in a 90% glycerol−water mixture (volume to volume). The glycerol volume was measured by weight using the glycerol density of 1.261 g/mL. The iodoacetamido derivatives of xanthene dyes were first dissolved at high concentration in DMF and then added to buffer or water in the desired final concentration. The protein buffer is 50 mM Tris-HCl at pH 8 and 0.2 mM PMSF.

Preparation and Labeling of Myosin Subfragment 1. Rabbit myosin was prepared by a standard method (Tonomura et al., 1966). S1 was prepared by digesting myosin filaments with α-chymotrypsin (Weeds & Taylor, 1975). The 5′IATR, 5′IAF, or IAA treatment of S1 was performed with a 1.2−1.0 (or 10−1.0 for IAA) dye−protein ratio (corresponding to 120 μM dye) in 50 mM TES buffer at pH 7.0 with 0.2 mM PMSF (labeling buffer) and 4 °C for 12 h. The reaction was stopped by separating the modified proteins from the unreacted dye on a Sephadex G-25 column equilibrated with protein buffer. The protein was further dialyzed in this buffer overnight. The specificity of 5′IATR, 5′IAF, or IAA for SH1 on S1 was characterized as described previously (Ajtai & Burghardt, 1989, 1992; Ajtai et al., 1992).

The time dependence of the probe labeling of S1 was monitored by observation of its CD signal. S1 in 70 μM concentration was incubated with a 1.5−1.0 5′IATR−protein ratio in labeling buffer at 4 °C. The reaction was followed in the cuvette of the spectropolarimeter.

Spectroscopic Measurements and Data Fitting. We measured absorption on a Beckman DU650 (Beckman Instruments, Fullerton, CA) or a Cary 4 (Varian Instruments, Houston, TX) spectrophotometer and circular dichroism (CD) on a Jasco J-720 spectropolarimeter (Jasco Inc., Tokyo, Japan). Spectral resolution was 1 nm. We measured fluorescence on an SLM 8000 spectrofluorometer (SLM Instruments, Urbana, IL). Fluorescence emission spectra were recorded with monochromator slits of 2 nm. Tryptophan excitation spectra from labeled and unlabeled S1 were recorded with an emission wavelength of 370 nm; emission spectra were recorded with an excitation wavelength of 295 nm. Tyrosine excitation spectra were recorded with an emission wavelength of 303 nm. All measurements were made in the steady state at 6 °C.

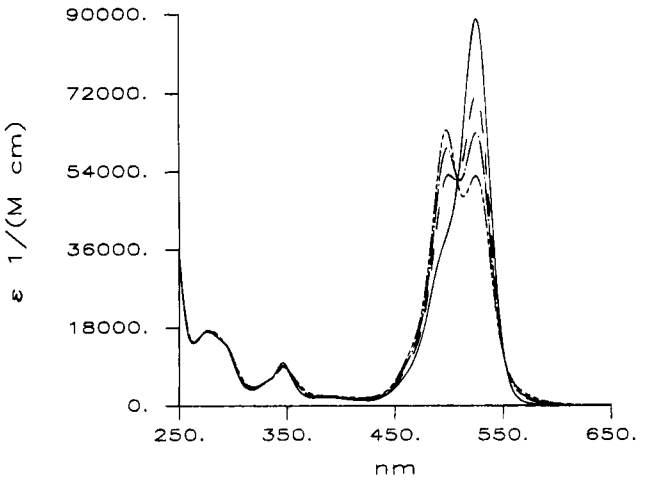

FIGURE 1: Effective extinction coefficient of R6G in water for dye concentrations of 0.01 (—), 0.10 (- - -), 0.20 (—·—), and 0.40 (- - —) mM.

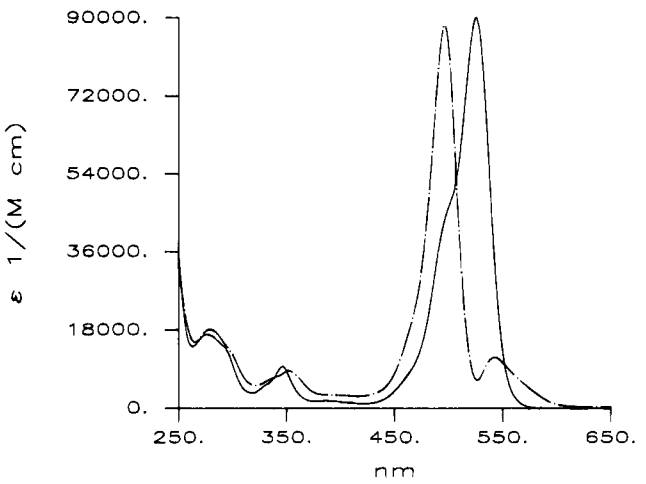

FIGURE 2: Monomer (—) and one-half times the dimer (—·—) extinction coefficients for R6G.

When necessary, we fitted spectral curves with weighted Gaussian line shapes using a method combining linear and nonlinear curve fitting. The spectral intensities are the linear parameters directly proportional to dipole or rotary strengths for different electronic transitions. Wavelength maxima and transition bandwidths are the nonlinear parameters.

Molecular Modeling. The structures of the monomeric dyes and the small peptides containing tryptophan were surmised by energy minimization in vacuum using the molecular modeling software HyperChem (Hypercube Inc., Waterloo, Ontario, Canada).

RESULTS

(A) Absorption from Rhodamine, Fluorescein, Tryptophan, 5'R-S1, and 5'F-S1. We measured the absorption from four solutions containing 0.01, 0.10, 0.2, and 0.4 mM concentrations of rhodamine dye to estimate the association constant and the extinction coefficients of the monomer and dimer species by the methods outlined in part I. Figure 1 shows the effective extinction coefficient, $\epsilon = A/([M_0]/)$, where $[M_0]$ is the initial concentration of dye and / the optical path length of R6G for different $[M_0]$'s. There the broadening and splitting of the absorption bands as a function of dye concentration indicate dimer formation. Figure 2 shows the surmised extinction coefficients for the monomer and dimer species of R6G. We similarly considered absorption spectra from the dimer species of RB, 5'IATR, and the heterodimer of R6G-RB. We fitted the extinction coefficients with weighted Gaussian line shapes to estimate the energy and dipole strength of the three lowest energy transitions in the monomer and the six lowest energy transitions in the dimer. The absorption bands were not usually single Gaussians, and only the two lowest energy transitions of the dimer were cleanly separated. In all cases the sum of dipole strengths for the dimer transitions nearly equaled twice the sum of the dipole strengths of the monomer species as required by the exciton theory coupling the dipole oscillators.

We measured the extinction coefficient of 5'IAF in protein buffer and TME in water (data not shown) to estimate the transition energies and dipole strengths. TME is a model compound for tryptophan in a protein. Valeur and Weber (1977) estimated the shapes of the $^1A \rightarrow {}^1L_a$ and $^1A \rightarrow {}^1L_b$ transitions in tryptophan. We used these shapes for the $^1A \rightarrow {}^1L_a$ and $^1A \rightarrow {}^1L_b$ and two more Gaussians for the $^1A \rightarrow {}^1B_a$ and $^1A \rightarrow {}^1B_b$ transitions to estimate the contributions of these four transitions to the spectrum of TME. We estimated the transition energy from the weighted average wavelength in the absorption bands.

We measured the extinction coefficients of 5'R-S1 and 5'F-S1 in protein buffer (data not shown). We fitted these spectra with weighted Gaussian line shapes to estimate the energy and dipole strength of four transitions in the 5'IATR and two in the 5'IAF when modifying S1.

Table 1 summarizes the physical properties surmised from the absorption measurements of these compounds.

(B) Fluorescence Anisotropy from Rhodamine, 5'IAF, 5'R-S1, 5'F-S1, and Tryptophan. We measured the excitation fluorescence anisotropy spectra from R6G, RB, 5'IATR, and 5'IAF monomers and from R6G dimers as reported elsewhere (Burghardt et al., 1995). These measurements indicate the relative orientation of the absorption and emission dipoles of the molecule or complex and are important constraints for the coupled dipole oscillator calculation of dimer conformation (see eq 25 from part I).

Observation of the fluorescence anisotropy from the immobilized monomers was carried out in 90% glycerol solution at $T = 0$ °C. Using a dye concentration of 0.5–1.0 μM ensured that only the monomer species was present. We observed the fluorescence anisotropy from the dimer species of R6G under quite different conditions and using a modified fluorescence cuvette as described elsewhere (Burghardt et al., 1995).

The lowest energy transitions of indole are designated $^1A \rightarrow {}^1L_a$ and $^1A \rightarrow {}^1L_b$. Yamamoto and Tanaka (1972) showed that their absorption dipoles lie within the plane of the indole and are oriented at −38° and 56° to the long axis of the molecule, respectively. Valeur and Weber (1977) measured the anisotropy from immobilized tryptophan and showed that under our experimental conditions all emission occurs from the ^1L_a transition band with limiting anisotropy, $r = 0.3$. We used published semiempirical calculations of indole electronic dipole transition moments to orient the two higher energy transitions, $^1A \rightarrow {}^1B_a$ and $^1A \rightarrow {}^1B_b$, within the indole ring (Goux et al., 1976; Ilich & Prendergast, 1992). We assume that they too emit through the ^1L_a emission dipole.

The fluorescence anisotropies from rhodamine monomers and dimers, 5'IAF, 5'R-S1, 5'F-S1, and tryptophan are summarized in Table 2. The values listed for 5'R-S1 and

Table 1: Physical Quantities Measured from Rhodamine, Fluorescein, and Tryptophan[a]

row	symbol	5′IATR	5′IATR dimer B	5′IATR dimer A	R6G	RB	R6G−RB	5′R-S1	5′IAF	5′F-S1	TME
1	K	6700 ± 70			1800 ± 30	800 ± 30	4300 ± 30				
2	e_1	538.6			512.2	537.9			493.6		264.2
3	e_2	385.7			391.6	395.0					262.3
4	e_3	354.9			345.1	349.7			336.1		217.3
5	e_4										195.0
6	E_1	558.4 (557.6)	557.6	577.0	545.7 (543.7)	564.3 (561.1)	580.2 (572.3)	548.7 (568.4)		502.3 (499.8)	
7	E_2	506.5 (508.5)	522.9	508.5	489.6 (484.4)	513.9 (511.1)	511.7 (485.2)	502.4 (522.9)			
8	E_3, E_4	409.8 (383.8)	384.5	383.3	387.8 (390.1)	405.0 (390.7)	400.9 (394.8)	(n/c)			
9	E_5	358.1 (355.3)	356.6	355.2	351.7 (344.7)	358.1 (350.8)	350.1 (349.7)	351.9 (356.8)		350.3 (336.7)	
10	E_6	351.7 (352.6)	352.6	354.2	331.3 (338.9)	342.6 (346.9)	338.8 (344.8)	309.8 (355.4)			
11	$D^{M}_{0,1}$	34.5			61.7	57.5			43.9		4.9
12	$D^{M}_{0,2}$	7.4			1.2	6.1			0.		2.5
13	$D^{M}_{0,3}$	2.7			5.7	3.5			9.4		16.3
14	$D^{M}_{0,4}$										26.7
15	D^{M}_{T}	44.6			68.6	67.1			53.3		50.4
16	$D^{C}_{0,1}$	31.2 (34.1)	70.0	0.0	16.1 (23.4)	24.2 (26.9)	4.4 (2.0)	51.4 (62.7)		39.6 (40.0)	
17	$D^{C}_{0,2}$	30.1 (33.5)	0.0	65.3	92.0 (97.8)	83.0 (84.1)	102.8 (118.8)	11.1 (0.0)		0 (0)	
18	$D^{C}_{0,3} + D^{C}_{0,4}$	20.4 (15.4)	12.5	18.1	13.6 (3.1)	14.0 (16.6)	9.4 (6.9)	(n/c)		0 (0)	
19	$D^{C}_{0,5}$	9.0 (3.2)	0.4	5.8	8.0 (1.7)	4.3 (4.7)	8.0 (4.6)	15.5 (0.5)		10.9 (8.6)	
20	$D^{C}_{0,6}$	0.0 (3.0)	6.3	0.0	2.6 (11.3)	3.9 (1.9)	0.0 (3.5)	6.7 (3.3)		0 (0)	
21	D^{C}_{T}	90.7 (89.2)	89.2	89.2	132.3 (137.3)	129.4 (134.2)	124.6 (135.8)	84.7 (66.5)		50.5 (48.6)	

[a] Row 1 is the association constant, K, for dimer formation in units of M^{-1}. Rows 2−10 are transition energies for monomers (2−5) and dimers or complexes (6−10) expressed by wavelength in nanometers. Rows 11−21 are dipole strengths expressed in debye^2 for monomers (11−14) and dimers or complexes (16−20) and summed dipole strengths (15 and 21). Quantities in parentheses are theoretical values computed by applying the exciton theory (Burghardt & Ajtai, 1995). The dimer species of rhodamine are described in terms of six transitions; however, the third and fourth transitions were not independently resolved so that individual energies are not known and their dipole strengths are summed. Exciton theory conserves dipole strengths so that two times the sum of the monomer dipole strengths should equal the sum of the dimer dipole strengths (compare rows 15 and 21). This holds approximately for all species. When more than one Gaussian is used to approximate an absorption band, the dipole strengths are summed and the transition energy is computed as a weighted average with weights given by the dipole strength. When treating rhodamine dimers in solution, three monomer transitions and six dimer transitions were considered in the coupled oscillator calculation. When the rhodamine dimer interacts with tryptophan in 5′R-S1, the two-molecule formalism is used by treating the dimer as a single molecule interacting with tryptophan. In this case four transitions of the individual molecules and eight transitions of the complex were estimated in the coupled dipole calculation. Experimentally, we observed quantities from only the four lowest energy 5′R-S1 transitions that could be compared with their theoretical values. The transitions around 400 nm in the 5′R-S1 were not considered (labeled n/c in the table) in the calculation because they were small compared to the other four transitions and including them would have dramatically increased the required computation time. When 5′IAF interacts with tryptophan in 5′F-S1, two transitions from the individual molecules and four transitions of the complex were estimated in the coupled dipole calculation. Experimentally, we observed quantities from only the two lowest energy 5′F-S1 transitions that could be compared with their theoretical values. Random errors are accounted for in the calculation by expecting all energies to be correct to within 10 nm and dipole strengths to within 10%.

Table 2: Fluorescence Anisotropy Measured from Immobilized Rhodamine, Fluorescein, and Tryptophan for the Transitions Listed in Table 1[a]

row	symbol	5′IATR	5′IATR dimer B	5′IATR dimer A	R6G	RB	R6G−RB	5′R-S1	5′IAF	5′F-S1	TME
1	r^{M}_{1}	0.333			0.370	0.370			0.33		0.300
2	r^{M}_{2}	−0.077			0.112	0.060					−0.130
3	r^{M}_{3}	−0.113			−0.124	−0.131			−0.10		0.038
4	r^{M}_{4}	−0.050									0.027
5	r^{C}_{1}	0.328 (0.328)	0.328	0.328	0.370 (0.370)	n/o (0.370)	n/o (0.370)	0.328 (0.328)		0.331 (0.331)	
6	r^{C}_{2}	0.328 (0.320)	0.328	0.320	0.370 (0.365)	n/o (0.370)	n/o (0.370)	0.328 (0.328)			
7	r^{C}_{3}, r^{C}_{4}	−0.079 (−0.027)	−0.035	−0.022	0.080 (0.111)	n/o (0.062)	n/o (0.043)	(n/c)			
8	r^{C}_{5}	−0.126 (−0.137)	0.212	−0.164	−0.080 (−0.076)	n/o (−0.057)	n/o (−0.168)	−0.120 (−0.11)		−0.10 (−0.16)	
9	r^{C}_{6}	−0.126 (−0.108)	−0.108	−0.142	−0.050 (−0.0137)	n/o (−0.151)	n/o (−0.031)	−0.072 (−0.02)			

[a] Rows 1−4 are the anisotropies for monomer species, and rows 5−9 are for dimer or complexed species. The numbers in parentheses indicate the values for the anisotropies computed for the complexed probes using the exciton theory. The anisotropies of some of the dimer species were not observed (labeled n/o in the Table).

5′F-S1 were taken from previous work (Ajtai et al., 1992; Ajtai & Burghardt, 1992).

(C) Structure of the Rhodamine Dimers in Solution. We applied the coupled dipole oscillator theory to account for the absorption and fluorescence anisotropy data in Tables 1 and 2 to surmise the structure of the rhodamine dimers in solution. NMR studies of the structure of the homodimers of R6G and RB and the heterodimers of R6G and RB indicate that each dimer has antiparallel stacked xanthene rings separated by 3.0−3.6 Å (Ilich et al., 1995). We assume

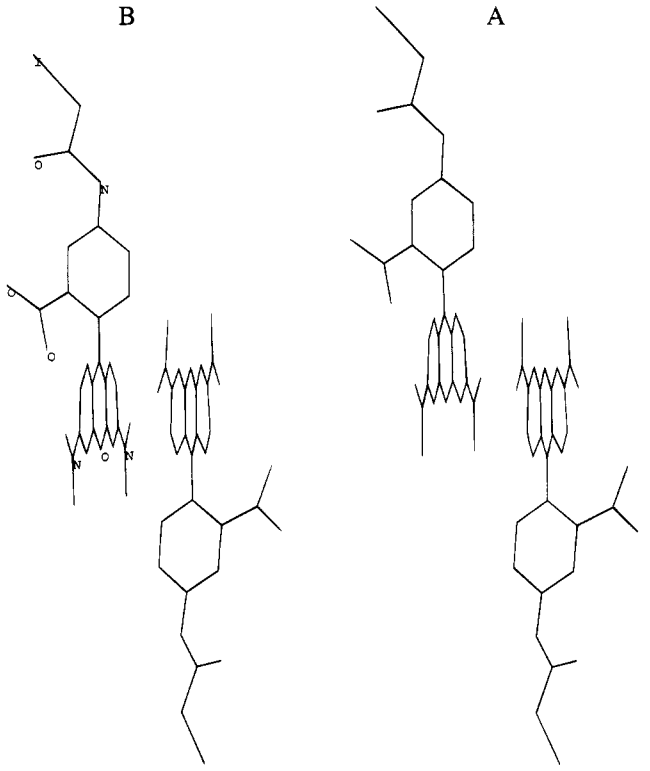

FIGURE 3: Two structures of the 5'IATR dimer. Structure A (right) has an extended conformation and a forbidden electronic transition from its lowest energy state. Structure B (left) has a more compact conformation and an allowed electronic transition from its lowest energy state. Structure B is the conformation imposed on the dimer by the binding site of S1.

that the same structure and constraints hold for the 5'IATR dimers. Within these constraints the antiparallel monomers are allowed to slide relative to each other in parallel planes to accommodate the observed spectroscopic parameters. Comparisons between the observed and calculated parameters are shown in Tables 1 and 2.

We find that the three homodimers, made from R6G, RB, or 5'IATR, have a common characteristic in that they appear to form in two distinct conformations. One conformation, dimer structure A, is characterized by its larger size due to xanthene ring stacking that is staggered like a stair case (J-type structure; Xu & Neckers, 1987) and by its lowest energy electronic transition that is forbidden. This dimer form has been observed previously under quite different conditions and is identified by its low quantum efficiency for fluorescent emission (Chambers et al., 1974). The other conformation, dimer structure B, is more compact due to the larger overlap of the surface of the xanthene planes (H-type structure; Xu & Neckers, 1987). The lowest electronic transition of structure B is an allowed transition. This dimer form is identified by its high quantum efficiency for fluorescent emission. In the ground state at equilibrium the two dimer forms evidently interconvert because the extinction coefficient shows evidence of both forms. An excited-state isomerization reaction may also occur, permitting an excited dimer A to emit a photon by converting to dimer B. This mechanism would allow dimer A to efficiently fluoresce (Burghardt et al., 1995). Figure 3 shows the proposed structure of the two dimer forms of 5'IATR. The two dimer conformations of 5'IATR appear to be detected when these forms modify myosin S1. These data are discussed in Results, section G.

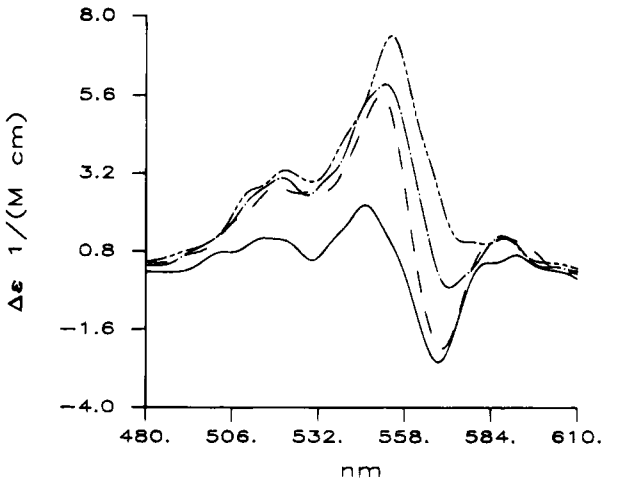

FIGURE 4: Time-dependent CD extinction coefficient from 5'R-S1 at 3 min (—), 30 min (- - -), 2 h (—·—), and 18 h (- - —) following the initiation of the reaction between the 5'IATR dimer and S1.

Although each homodimer species has two populations of structurally different dimers at equilibrium, the partition coefficient is species dependent. The 5'IATR dimers are equally likely to form structures A and B, while the R6G dimer is an 81% to 19% split, and the RB dimer is a 77% to 23% split. The heterodimer made up of R6G and RB shows little evidence of the dimer B form.

(D) CD from Tryptophan, 5'R-S1, and 5'F-S1. The near-UV circular dichroism signal from tryptophan in a protein originates from the coupling of the indole absorption dipoles with the magnetic dipole of the carbonyl in the peptide backbone of the protein (Nielsen & Schellman, 1967; Schellman & Nielsen, 1967; Bayley et al., 1969; Hooker & Schellman, 1970). The amplitude and sign of the tryptophan CD signal depend on the relationship of the coupled magnetic and electric dipoles, i.e., on the tertiary structure of the protein. The CD extinction coefficient from TME in water measured as a model compound for tryptophan in a protein (data not shown). We fitted this spectrum assuming line shapes obtained from the extinction coefficient fit, thereby allowing an estimate of the rotary strength contributed by each transition. We estimated a lower limit for the tryptophan magnetic dipole moment amplitude from its rotary strength, computed from the CD extinction coefficient employing eq 15 from part I, with the assumption that the magnetic and electric dipole moments are parallel.

5'IATR and 5'IAF do not have CD signals while free in solution because the molecules do not possess a magnetic dipole and because the formation of positive or negative chirality conformers is equally likely. When covalently attached to S1, however, a complex time-dependent CD signal appears in the absorption band of the 5'IATR, indicating that the bound probe is chiral. Shown in Figure 4 is the time development of the CD extinction coefficient when 5'IATR modifies S1. Initially after mixing the 5'R-S1 CD signal has negative and positive phases. The final equilibrium signal, achieved after several hours, is positive. We will interpret these time-dependent signals in terms of the two 5'IATR dimer conformations described above in Results, section C. Figure 5 shows the equilibrium CD extinction coefficient spectrum from 5'R-S1 and 5'F-S1. In the presence of S1, a CD signal appears in the absorption band of the 5'IAF indicating that the bound probe is chiral

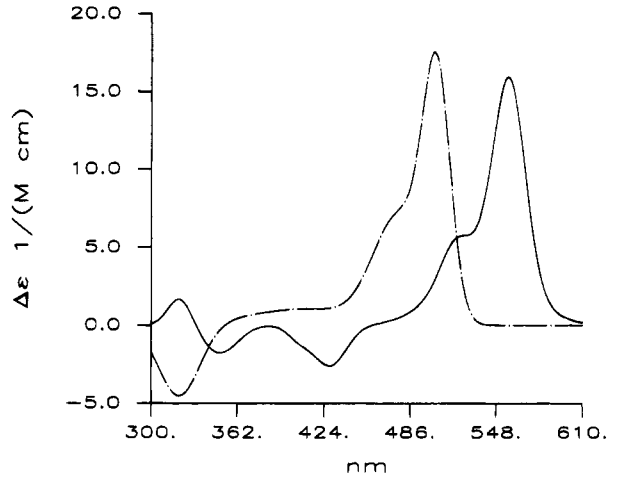

FIGURE 5: CD extinction coefficient for 5′F-S1 (—·—) and two times the quantity for 5′R-S1 (—). The CD spectrum for 5′R-S1 shows the splitting in the absorption bands at 330 nm due to the presence of the dimer form of the rhodamine.

when bound to SH1. The time dependence of the 5′F-S1 signal changes in amplitude but not in shape as the probe modifies SH1 (data not shown). The addition of MgATP at 6 °C did not change the shape or amplitude of the induced CD signal from either probe. The induced CD of the probe is characteristic to the native structure of the S1 since the signal is lost when probe-modified S1 is denatured.

We determined that the CD signal from 5′R-S1 originates from 5′IATR-modifying SH1 by attempting to label premodified S1. Iodoacetamide (IAA) is well-known to very specifically block SH1, and we used this compound to modify 95% of the SH1 groups in S1 (Ajtai & Burghardt, 1989). The extent of IAA modification of SH1 was measured by the inhibition of K^+-EDTA ATPase and activation of the Ca^{2+}-activated ATPase in the premodified S1. No CD signal at the 5′IATR absorbance band was observed from the premodified S1 in the presence of 5′IATR under the conditions used for 5′IATR labeling of S1, indicating that the blocking of 5′IATR modification of SH1 completely inhibits the generation of the CD signal. An experiment with 5′IAF replacing 5′IATR gave identical results. The specificity of the induced CD signal for SH1 modification suggests that it may be useful to follow the reaction kinetics of SH1 modification and potentially as a sensor for local structural changes in S1.

Figure 5 compares the equilibrium CD extinction coefficients of 5′R-S1 and 5′F-S1. The 5′IATR CD absorption band centered at 330 nm is split into positive (blue shifted) and negative (red shifted) amplitude transitions, indicating that the signal originates from a dimer. In absorption the two bands overlap sufficiently to give the appearance of one transition. 5′F-S1 shows no splitting in this transition band (see Figure 5) and is known to modify S1 in a one-to-one stoichiometry (Takashi, 1979).

The origin of the CD signal in the rhodamine absorption band of 5′R-S1 can be the dimer itself, since coupled oscillators can give rise to CD (Tinoco, 1960, 1961; Bayley et al., 1969) and/or the dimer interacting with a chiral residue such as tryptophan in the SH1 binding site. The CD signal from 5′F-S1 could only be from the probe interacting with chiral residues, as in the case of the fluorescein−antifluorescein antibody complex (Tetin et al., 1992), or like the optically active amines in the chiral enantioselective complexing agents for bilirubin (Lightner et al., 1987, 1988). Aromatic residues are probable candidates since, with other factors being equal, they couple most strongly with the dyes. Evidence supporting the notion that the origin of the CD signal is a tryptophan−probe interaction is discussed further in the next section.

Table 3: Rotational Strengths in Debye Bohr Magnetons Measured from 5′R-S1, 5′F-S1, and Tryptophan for the Transitions Listed in Table 1[a]

row	symbol	TME	5′R-S1 initial (approx)	5′R-S1 equilibrium	5′F-S1 equilibrium
1	$R^M_{0,1}$	0.017			
2	$R^M_{0,2}$	0.012			
3	$R^M_{0,3}$	0.070			
4	$R^M_{0,4}$	−0.030			
5	$R^C_{0,1}$		−0.047 (−)	0.13 (+)	0.29 (+)
6	$R^C_{0,2}$		0.093 (+)	0 (0)	0 (0)
7	$R^C_{0,3}$			(n/c)	0 (0)
8	$R^C_{0,4}$			(n/c)	0 (0)
9	$R^C_{0,5}$			−0.016 (−)	−0.10 (−)
10	$R^C_{0,6}$			0.011 (+)	0 (0)

[a] Rows 1−4 are the rotary strengths of the lowest energy transitions in the TME model for tryptophan. Rows 5−10 are the rotary strengths of the complexed probe. Only the two lowest energy bands were observed from the time-dependent CD signal from 5′R-S1. The sign and order of magnitude of computed rotary strengths are compared with observed values to judge the goodness of fit (because we can estimate only the lower limit of the magnetic dipole moment for tryptophan from its rotary strength). The signs in parentheses indicate the signs of the rotary strengths computed for the complexed probes using the exciton theory.

Table 3 summarizes our measurement of the rotary strengths of several of the lowest energy absorption bands of TME, 5′R-S1, and 5′F-S1.

(E) Fluorescence Intensity Measurements of 5′R-S1 and 5′F-S1. If a chiral aromatic residue in SH1 interacts with the rhodamine dimer or fluorescein monomer modifying SH1 to cause the observed CD signal, we expect energy transfer to occur from this residue to the dye by the Förster mechanism of fluorescence resonance energy transfer (FRET) or an alternative mechanism (Förster, 1965). We investigated the efficiency of energy transfer from the tyrosines and tryptophans of S1 to 5′IATR and 5′IAF by observing the fluorescence intensity from these residues in the presence and absence of the probe.

We prepared two identical samples of S1 and labeled one with 5′IATR or 5′IAF by the protocol described in Materials and Methods. The other sample, the unlabeled S1, was prepared identically to the labeled sample except no dye was introduced to the S1. In some experiments unreacted probe was removed from the labeled S1 sample by dialysis; in others the unreacted dye was not removed. We compared the fluorescence intensities of labeled and unlabeled S1. Figure 6 shows the excitation spectrum from equal protein concentrations of 5′R-S1 and unmodified S1 with emission collected at 370 nm. At 300 nm excitation and 370 nm emission, tryptophan is detected exclusively, and the ratio of the fluorescence intensities for 5′R-S1 and S1, $F_{5'R\text{-}S1}/F_{S1}$, = 0.74. Identical data were obtained for 5′F-S1. The difference between the spectra shown in Figure 6 has the shape typical for tryptophan excitation, suggesting that the

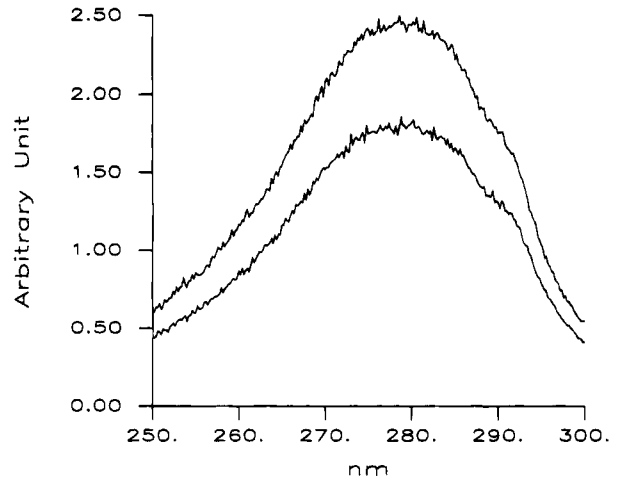

FIGURE 6: Fluorescence excitation spectra from S1 (top) and 5′R-S1 (bottom). Fluorescence emission is collected at 370 nm from tryptophan residues in S1. Identical protein concentrations are compared in the two curves so that the decrease in intensity from the labeled sample is due to energy transfer from tryptophan to the 5′IATR dimer.

missing energy in the 5′R-S1 spectrum is transferred to the probe. We also measured the excitation spectrum from equal protein concentrations of 5′R-S1 and unmodified S1 with emission collected at 303 nm (data not shown). At this emission wavelength tyrosine is detected preferentially, and the ratio of the fluorescence intensities for 5′R-S1 and S1, $F_{5'R\text{-}S1}/F_{S1}$, = 0.86. Again, identical data were obtained for 5′F-S1. The difference between the tyrosine excitation spectra for labeled and unlabeled S1 has a shape typical for tyrosine excitation, suggesting that the missing energy is transferred to the probe. The presence or absence of unreacted dye in the labeled S1 samples has no effect on the intensity ratios.

The quenching of tryptophan fluorescence by energy transfer suggests that at least one of the tryptophans in S1 is within ~25 Å (the characteristic transfer distance from tryptophan to rhodamine or fluorescein) of the 5′IATR dimer or 5′IAF. The 5′IAF and the indole side chain extend at most ~10 and ~5 Å from the α-carbon backbone, respectively, so that a tryptophan within ~40 Å of SH1 is a potential candidate for energy transfer to the probe. The crystallographic structure of S1 indicates that Trp510, Trp113, Trp131, and Trp595 are within 40 Å of SH1. The quenching of tyrosine fluorescence by energy transfer also suggests that more than one of the tyrosines in S1 are within ~25 Å (the characteristic transfer distance from tyrosine to rhodamine or fluorescein) of the 5′IATR dimer or 5′IAF. The crystallographic structure of S1 indicates that there are many tyrosines throughout S1 so that there are many candidate residues. On the basis of the FRET data we would look for residues where energy transfer could occur from both tryptophan and tyrosine to the probe. We have, however, more information about the probe−protein conformation to narrow down our search as described below.

(F) Structure of the 5′F-S1 and 5′IATR Dimer−S1 Complex Surmised from Exciton Theory and from the Orientation of the Probe Dipoles in the PHF of S1. We applied the exciton theory to the problem of the fluorescein−protein conformation (see part I). We coupled the two lowest energy transition dipoles in the fluorescein to the two lowest energy transition dipoles in tryptophan. The exciton calculation quantitatively accounts for the dipole strength, transition energy maximum, fluorescence anisotropy, and rotary strength from the complex. Just the sign and order of magnitude of the computed rotary strength are required to agree with the observed value because we estimate only the lower limit of the magnetic dipole moment in tryptophan from the model spectra. The numerical results of this computation are summarized in Tables 1−3 where the observed spectroscopic parameters are compared with the best fitting computed values. The fluorescein−tryptophan complex accounts quantitatively for all of the spectroscopic parameters observed for 5′F-S1 and gives a separation distance between the molecules in the complex of ~3.3 Å; i.e., the separation distance is near the van der Waals distance. We also used the exciton theory to couple the two lowest energy transition dipoles in the fluorescein to the two lowest energy transition dipoles in tyrosine. We found that a fluorescein−tyrosine complex could not quantitatively account for the hypochromic effect observed for fluorescein binding to S1 because the tyrosine electric dipole moment is too small.

The results from the coupled dipole calculation suggest that the fluorescein−S1 interaction involves the close association of fluorescein and tryptophan. The close fit excludes from consideration all of the tryptophans except Trp510. This is consistent with the FRET data because the fluorescein will completely quench Trp510 emission and is near enough to several tyrosines to account for the observed energy transfer from tyrosine to fluorescein.

Several fluorescein−tryptophan conformations accounted for all of the observed spectroscopic parameters equally well. We narrowed the field of plausible fluorescein−tryptophan conformations using the known relationship between the probe dipole and the PHF of S1. We estimated the orientation of the lowest energy absorption and emission dipoles of the rhodamine dimer probe in the PHF of S1 using our method based on the analysis of data from multiple probes (Burghardt & Ajtai, 1994; Ajtai et al., 1994). The 5′IAF probe of S1 gives similar fluorescence polarization ratios to rhodamine when labeling muscle fibers so that we assume for our purpose here that the fluorescein and the rhodamine are oriented similarly in the PHF of S1 (Ajtai & Burghardt, 1992). We located the PHF of S1 from the α-carbon structure of S1 by the method outlined in part I and searched through the candidate fluorescein−tryptophan conformations, best fitting the spectroscopic parameters, while conforming to the constraints relating the orientation of the probe to the PHF of S1.

We performed the identical calculations to find candidate steady-state 5′IATR dimer−tryptophan conformations. We used the 5′IATR dimer B form (the compact dimer conformation) and assumed that it interacted exclusively with Trp510. The comparison of observed and calculated spectroscopic parameters is summarized in Tables 1−3. The set of best fitting 5′IATR dimer−tryptophan conformations was subjected to the same probe orientation constraints as the fluorescein−tryptophan complex. By pooling the conformations of fluorescein−tryptophan and steady-state 5′IATR dimer−tryptophan, we found one solution for all of the imposed constraints that also had a similar Trp510 conformation relative to the protein backbone. Figure 8 shows our best estimates for the conformations for 5′F-S1 and 5′IATR dimer−S1.

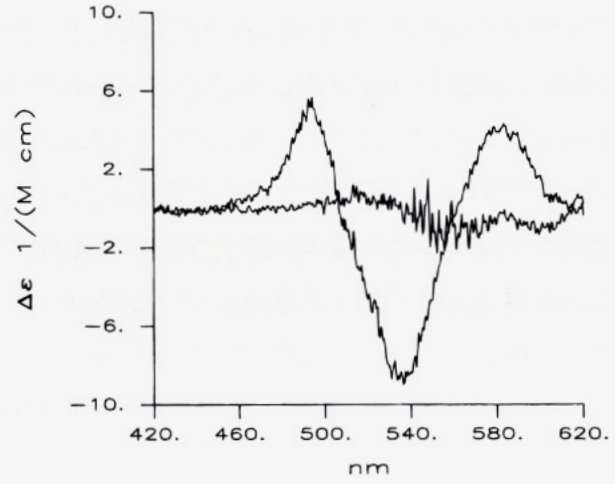

FIGURE 7: CD extinction coefficients for R6G (large amplitude) and RB noncovalently interacting with S1.

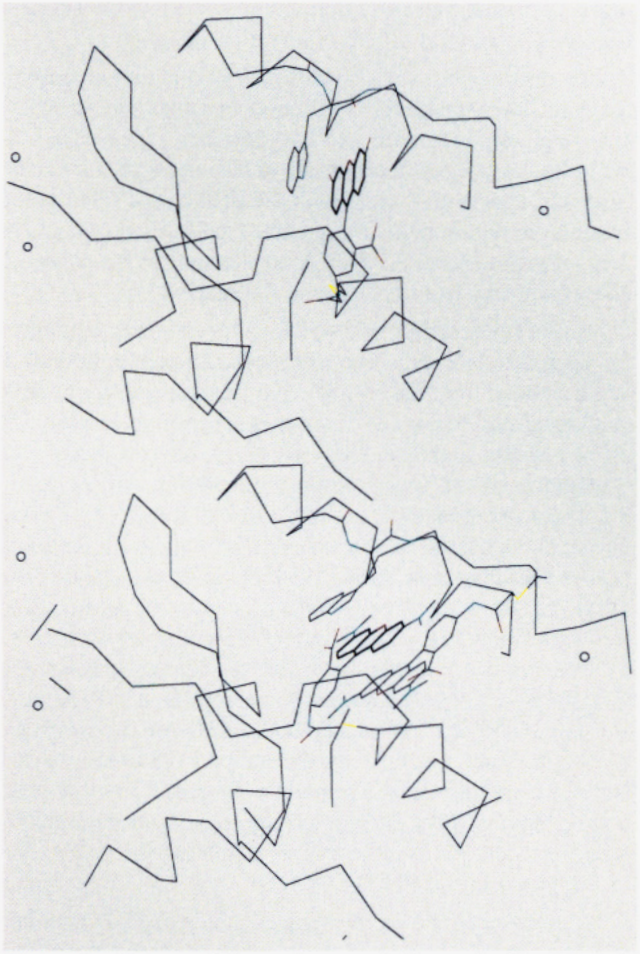

FIGURE 8: Close-up of the probe−protein interaction involving the 5′IAF (top) or 5′IATR dimer (bottom) and the indole of Trp510. The dimer conformation is the compact, dimer B form shown in Figure 3.

(G) Time-Dependent 5′IATR Dimer−S1 Complex Surmised from Exciton Theory. The time-dependent CD signal from 5′IATR-modifying S1, shown in Figure 4, suggests a mechanism for the probe modification of S1 that involves the two rhodamine dimer forms A and B. Initially, both forms readily modify SH1 so that the negative and positive phases of the CD signal originate from the linear combination of signals from both of the 5′IATR dimer forms A and B, respectively. The early time CD signal indicates that there is light absorption at ~580 nm where only dimer A has a transition. This lowest energy transition in dimer A has zero dipole strength (see Table 1); however, perturbations caused by fitting into the SH1 binding pocket or from interaction with Trp510 or other aromatic residues could cause the remixing of electronic states permitting significant absorption. The light absorption indicated by the final, steady-state CD signal in the protein resembles that characteristic to dimer B in energy and dipole strength. Figure 3 shows the extended and compact conformation of dimers A and B, respectively. The chemical modification of SH1 by either dimer form appears to be equally likely, but subsequently the SH1 bonding pocket preferentially converts dimer A to dimer B.

(H) CD from Noncovalent Probes of S1. We studied the noncovalent binding of rhodamine probes to S1 by observing the induced CD signal from the probe−protein complex in solution. None of the probes exhibit a CD signal when free in solution as expected from symmetry. Shown in Figure 7 are CD signals from R6G and RB interacting with S1. These dyes differ structurally from the 5′IATR by more extensive methylation. Only the R6G had a detectable signal that was completely reversible upon removal of the dye. Evidently, the R6G, but not the RB, specifically interacts with the S1. The R6G signal changes sign twice within the dimer absorption band, suggesting that R6G binds at two or more sites on S1. Modification of SH1 with IAA did not affect the R6G CD signal from S1.

The addition of RB to 5′R-S1 changes the CD signal, indicating that RB was able to interact with the 5′IATR dimer at SH1. The addition of R6G to 5′R-S1 also changes the CD signal to a form that is not equal to the sum of the CD signals for these dyes interacting separately with S1 (data not shown). Upon removal of either noncovalent dye the characteristic 5′R-S1 signal reappeared. It is unlikely that a heterodimer made up of one 5′IATR and one R6G or RB molecule formed because the characteristic 5′R-S1 signal always reappeared upon removal of the noncovalent dye. This is not surprising since the affinity of 5′IATR for itself was considerably higher than that of any of the other probes (see Table 1). It seems plausible that both RB and R6G can interact with the 5′IATR dimer on S1 while the R6G also binds to one or more separate sites on S1.

DISCUSSION

The coupling of free energy from ATP hydrolysis in myosin to work production in muscle is accomplished by intramolecular events in myosin related to communication between the ATPase and actin binding sites and with intermolecular events related to the rotation of the myosin cross-bridge relative to actin. Direction-reporting fluorescent probes of myosin respond to both local and global changes in cross-bridge conformation and have the potential for providing information on both processes. The interpretation of probe signals in terms of global changes in cross-bridge attitude depends on the determination of the relationship between the probe dipoles and the PHF of S1, something that can be done in the absence of detailed knowledge of the probe−protein interaction. On the other hand, the interpretation of probe signals in terms of local changes in cross-bridge conformation *only* depends on the probe−protein interaction.

The rhodamine and fluorescein probes of S1 provide a variety of spectroscopic signals related to the local interactions of the probe with the protein. Rhodamine is a notable probe of S1 because of the many implications for cross-bridge movement during contraction derived from its polarized emission while attached to SH1 in muscle fibers (Borejdo et al., 1979; Ajtai et al., 1994), however, the interpretation of signals from it are complicated because it binds to S1 as a dimer. We must first describe the conformation of the rhodamine dimer, i.e., the monomer−monomer conformation, before solving the probe−protein conformation problem. Fortunately, the study of monomer−monomer or probe−protein conformation requires similar spectroscopic analytical tools.

We observed the formation of dimers in three rhodamine dyes, R6G, RB, and 5′IATR, using absorption spectroscopy and determined the association constant and extinction coefficients for the monomer and dimer species. Present and previous work on the fluorescence emission from rhodamine dimers provided information on the fluorescence anisotropy of this system. These spectroscopic data were accounted for in terms of dimer conformation with a coupled dipole oscillator model of the monomer−monomer interaction (Burghardt & Ajtai, 1995). Proton NMR studies also provided spatial information on dimer structure (Ilich et al., 1995). The proposed dimer conformation satisfies the constraints of all of the available information. The 5′IATR dimer in solution appears to have the two conformations shown in Figure 3. Both 5′IATR dimer forms, A and B, are detected by the initial CD signal induced in the dimers when they bind to SH1 in S1. The steady-state CD signal from 5′R-S1 shows that the protein preferentially converts dimer A into dimer B.

With a defined rhodamine dimer structure and the simpler fluorescein structure we turned to the problem of the probe−protein conformation for these probes. Energy transfer data from 5′R-S1 and 5′F-S1 indicated certain qualitative features of the probe−protein interaction. These data showed that there were four tryptophans in S1 that were close enough to either probe to give the observed energy transfer from tryptophan and that there were several tyrosines within the characteristic distance for energy transfer. We measured the absorption, CD, and fluorescence anisotropy from 5′R-S1 and 5′F-S1 and used a coupled dipole oscillator model to quantify (i) changes in absorption maxima and strength, (ii) the rotary strength, and (iii) the fluorescence anisotropy of the probe upon binding to S1 in terms of the conformation of the probe−S1 interaction. The calculation indicated that, if a tryptophan was to induce the observed perturbations in the spectroscopic parameters of the probes, then the indole must be about a van der Waals distance from the probe xanthene ring and that a single tyrosine could not cause the observed spectroscopic perturbations. There is no cluster of several tyrosines in the vicinity of SH1 that could coordinate with the probe xanthene while Trp510 is the only tryptophan that could form a tight complex with the probe xanthene. The Trp510 residue is located within the characteristic energy transfer distance to several tyrosines so that this choice for perturbing residue is consistent with all of the observed spectroscopic data. The origin of a protein-induced CD signal in the fluorescein−antifluorescein antibody interaction, however, is attributed to tyrosine *and* tryptophan residues (Tetin et al., 1992).

FIGURE 9: α-Carbon structure of S1 from Rayment et al. (1993), the imbedded 5′IAF modifying SH1 and interacting with Trp510, and the coordinate axes representing the PHF of S1. The lengths of the PHF axes represent the relative values of the rotational diffusion constants of S1. The smaller diffusion constants are very nearly equal.

The coupled dipole oscillator model placed the probe and the indole in the tryptophan in a particular conformation; however, all of the spectroscopic parameters were consistent with several distinct probe−tryptophan conformations. We made use of additional information from work on the orientation of the rhodamine dimer in the PHF of S1 (Ajtai et al., 1994) and used our method for computing the position of the PHF in the α-carbon structure S1 to correctly orient the rhodamine dimer within S1 (Burghardt & Ajtai, 1995). We assumed for the purpose of this calculation, and with some justification judging from the similarity of the fluorescence polarization ratios in fibers (Ajtai & Burghardt, 1992), that fluorescein and rhodamine dipoles were oriented alike in S1. This combination of constraints produced a small set of probe−tryptophan conformations that contained only one solution in which the tryptophan maintains a similar relationship to the S1 backbone while associated with either the rhodamine dimer or the fluorescein. These conformations, shown in Figure 8, are proposed as the most likely probe−S1 conformations.

The atomic resolution probe−S1 conformation is a starting point for an investigation of intramolecular structural changes in the local environment of SH1 in S1. Notable earlier work established the neighborhood of SH1 as responsive to bound nucleotide or actin binding (Quinlivan et al., 1969; Duke et al., 1979; Burke et al., 1976; Botts et al., 1989; Hiratsuka, 1993). It is feasible, on the basis of the methods developed and applied here, that spectroscopic detection of nucleotide binding could be described quantitatively in terms of probe−S1 conformation alterations. With these methods we will attempt to describe energy transduction as a series of local conformational changes leading to work production.

Shown in Figure 9 is the PHF frame of S1. The z-axis of this reference frame is the longest line segment. If we

describe the shape of S1 as a bent solid cylinder, with the bend occurring where the long α-helix in the light chain binding neck region begins, then the z-axis of the PHF makes some angle with each cylinder axis. We wish to estimate these angles. Referring to the neck portion as domain 1 and the other as domain 2, we applied to PHF calculation to these separate domains and compared the z-axis of the domain generated PHF's to that from the whole S1. We found that the z-axis of the PHF from domain 1 makes an angle of 17° with that from all of S1. The domain-generated PHF's make an angle of 25° with each other. We showed previously that the PHF z-axis of S1 in muscle fibers in rigor binds at 87° relative to the actin filament, suggesting that domain 1 makes an angle of 70° relative to actin (Ajtai et al., 1994). The angle between the cross-bridge and the fiber axis in rigor, surmised by several different techniques, was assigned values in the 45−65° range (Reedy et al., 1965; Reedy, 1968; Holmes et al., 1980; Taylor et al., 1984; Milligan & Flicker, 1987; Peckham & Irving, 1989). If the 45−65° angular range indicated the orientation of domain 1, then the bent conformation of S1 reconciles these disparate findings on the relative orientation of S1 and actin.

ACKNOWLEDGMENT

We thank Dr. Sungjo Park for critically reading the manuscript. Dr. S. Venyaminov made some preliminary measurements for this study.

REFERENCES

Ajtai, K., & Burghardt, T. P. (1989) *Biochemistry 28*, 2204−2210.
Ajtai, K., & Burghardt, T. P. (1992) *Biochemistry 31*, 4275−4282.
Ajtai, K., Ilich, P. J. K., Ringler, A., Sedarous, S. S., Toft, D. J., & Burghardt, T. P. (1992) *Biochemistry 31*, 12431−12440.
Ajtai, K., Toft, D. J., & Burghardt, T. P. (1994) *Biochemistry 33*, 5382−5391.
Andreev, O. A., Andreeva, A. L., & Borejdo, J. (1993) *Biophys. J. 65*, 1027−1038.
Bayley, P. M., Nielsen, E. B., & Schellman, J. A. (1969) *J. Phys. Chem. 73*, 228−243.
Błoński, S. (1991) *Chem. Phys. Lett. 184*, 229−234.
Borejdo, J., Putnam, S., & Morales, M. F. (1979) *Proc. Natl. Acad. Sci. U.S.A. 76*, 6346−6350.
Borejdo, J., Assulin, O., Ando, T., & Putnam, S. (1982) *J. Mol. Biol. 158*, 391−414.
Botts, J., Thomason, J. F., & Morales, M. F. (1989) *Proc. Natl. Acad. Sci. U.S.A. 86*, 2204−2208.
Burke, M., Reisler, E., & Harrington, W. F. (1976) *Biochemistry 15*, 1923−1927.
Burghardt, T. P., & Ajtai, K. (1994) *Biochemistry 33*, 5376−5381.
Burghardt, T. P., & Ajtai, K. (1995) *Biophys. Chem.* (submitted for publication).
Burghardt, T. P., Ando, T., & Borejdo, J. (1983) *Proc. Natl. Acad. Sci. U.S.A. 80*, 7515−7519.
Burghardt, T. P., Lyke, J., & Ajtai, K. (1995) *Biophys. Chem.* (in press).
Chambers, R. W., Kijiwara, T., & Kearns, D. R. (1974) *J. Phys. Chem. 78*, 380−387.
Duke, J., Takashi, R., Ue, K., & Morales, M. F. (1976) *Proc. Natl. Acad. Sci. U.S.A. 73*, 302−306.
Förster, Th. (1965) in *Modern Quantum Chemistry* (Sinanoĥlu, D., Ed.) pp 93−137, Academic Press, New York.
Gál, M. E., Kelly, G. R.; & Kurucsev, T. (1973) *J. Chem. Soc., Faraday Trans. 2 69*, 395−402.
Goux, W. J., Kadesch, T. R., & Hooker, T. M. (1976) *Biopolymers 15*, 977−997.
Grajek, H., Żurkowska, G., Drabent, R., & Bojarski, C. (1986) *Biochim. Biophys. Acta 881*, 241−247.
Hellen, E. H., Ajtai, K., & Burghardt, T. P. (1995) *J. Fluoresc.* (in press).
Hiratsuka, T. (1993) *J. Biol. Chem. 268*, 24742−24750.
Holmes, K. C., Tregear, R. T., & Barrington Leigh, J. (1980) *Proc. R. Soc. London, B 207*, 13−33.
Hooker, T. M., & Schellman, J. A. (1970) *Biopolymers 9*, 1319−1348.
Huxley, H. E. (1969) *Science 164*, 1356−1366.
Huxley, A. F., & Simmons, R. M. (1971) *Nature (London) 233*, 533−538.
Ilich, P. J. K., & Prendergast, F. G. (1992) *Biopolymers 32*, 667−694.
Ilich, P. J. K., Mishra, P., Macura, S., & Burghardt, T. P. (1995) manuscript in preparation.
Lightner, D. H., Gawronski, J. K., & Wijekoon, W. M. D. (1987) *J. Am. Chem. Soc. 109*, 6354−6362.
Lightner, D. H., An, J.-Y., & Pu, Y.-M. (1988) *Arch. Biochem. Biophys. 262*, 543−559.
López Arbeloa, I., & Ruiz Ojeda, P. (1982) *Chem. Phys. Lett. 87*, 556−560.
Milligan, R. A., & Flicker, P. F. (1987) *J. Cell Biol. 105*, 29−39.
Nielsen, E. B., & Schellman, J. A. (1967) *J. Phys. Chem. 71*, 2297−2304.
Peckham, M., & Irving, M. (1989) *J. Mol. Biol. 210*, 113−126.
Quinlivan, J., McConnell, H. M., Stowring, L., Cooke, R., & Morales, M. F. (1969) *Biochemistry 8*, 3644−3647.
Rayment, I., Rypniewski, W. R., Schmidt-Bäse, K., Smith, R., Tomchick, D. R., Benning, M. M., Winkelman, D. A., Wesenberg, G., & Holden, H. M. (1993) *Science 261*, 50−58.
Reedy, M. K. (1968) *J. Mol. Biol. 31*, 155−176.
Reedy, M. K., Holmes, K. C., & Tregear, R. T. (1965) *Nature (London) 207*, 1276.
Rohatgi, K. K., & Mukhopadhyay, A. K. (1971) *Photochem. Photobiol. 14*, 551−559.
Schellman, J. A., & Nielsen, E. B. (1967) *J. Phys. Chem. 71*, 3914−3921.
Selwyn, J. E., & Steinfeld, J. I. (1972) *J. Phys. Chem. 76*, 762−774.
Takashi, R. (1979) *Biochemistry 18*, 5164−5169.
Taylor, K. A., Reedy, M. C., Córdova, L., & Reedy, M. K. (1984) *Nature (London) 310*, 285−291.
Tetin, S. Y., Mantulin, W. W., Denzin, L. K., Weidner, K. M., & Voss, E. W. (1992) *Biochemistry 31*, 12029−12034.
Tinoco, I. (1960) *J. Chem. Phys. 33*, 1332−1338.
Tinoco, I. (1961) *J. Chem. Phys. 34*, 1067.
Tonomura, Y., Appel, P., & Morales, M. F. (1966) *Biochemistry 5*, 515−521.
Valeur, B., & Weber, G. (1977) *Photochem. Photobiol. 25*, 441−444.
Weeds, A., & Taylor, R. S. (1975) *Nature (London) 257*, 54−56.
Xu, D., & Neckers, D. C. (1987) *J. Photochem. Photobiol. 40*, 361−370.
Yamamoto, Y., & Tanaka, J. (1972) *Bull. Chem. Soc. Jpn. 45*, 1362−1366.

BI951339E